miR-877-3p promotes TGF-β1-induced osteoblast differentiation of MC3T3-E1 cells by targeting Smad7

GUISONG HE[1,2], JIANMING CHEN[3] and DONG HUANG[1,2]

[1]Department of Orthopedics, The Third School of Clinical Medicine, Southern Medical University, Guangzhou, Guangdong 510000; [2]Department of Orthopedics, Guangdong Provincial Second People's Hospital, Guangzhou, Guangdong 510220; [3]Department of Orthopedics, The Central Hospital of Yongzhou City, Yongzhou, Hunan 425000, P.R. China

Abstract. MicroRNAs (miRNAs) are emerging as important regulators of various physiological and pathological processes and may serve key roles in the maintenance of bone homeostasis via effects on osteoblast differentiation. The aim of the present study was to define the role of miR-877-3p in osteoblast differentiation using MC3T3-E1 cells, an osteoblast precursor cell line. It was demonstrated using RT-qPCR analysis that miR-877-3p was gradually increased in MC3T3-E1 cells during the osteoblastic differentiation induced by transforming growth factor (TGF)-β1. Gain-of-function and loss-of-function experiments revealed that the overexpression of miR-877-3p promoted the osteoblastic differentiation of MC3T3-E1 cells, whereas depletion of miR-877-3p inhibited this process *in vitro* and *in vivo*. Bioinformatics analysis and validation experiments demonstrated that Smad7, which acts as a negative regulator of osteogenesis, was a target of miR-877-3p. Furthermore, the overexpression of Smad7 partially reversed the osteoblastic differentiation of MC3T3-E1 cells induced by miR-877-3p. In conclusion, the results of the present study suggest that the miR-877-3p/Smad7 axis is associated with the osteoblastic differentiation of MC3T3-E1 cells and may indicate a potential therapeutic approach for osteogenesis disorders.

Introduction

Bone homeostasis mainly relies on the balance between bone-forming cells (osteoblasts) and bone-resorptive cells (osteoclasts) (1). The imbalance between bone formation and resorption leads to skeletal diseases associated with progressive bone degeneration, such as osteoporosis. Osteoporosis is a disease characterized by lower than normal bone mass and greater than normal bone loss, and is associated with increased risk of bone weakness and fracture (2). Studies on osteoblastic differentiation may help elucidate the pathogenesis of osteoporosis.

Transforming growth factor (TGF)-β1 is a polypeptide member of the TGF family that is involved in cellular functions, including the control of cell growth, proliferation and differentiation (3). TGF-β1 can maintain postnatal bone mass by coupling bone resorption and bone formation (4). TGF-β1 favors osteoclast differentiation by binding to a receptor on osteoclasts, and thereby activating Smad2/3, which is directly associated with the TRAF6-TAB1-TAK1 complex (5).

The possible mechanisms of osteoblastic differentiation and bone formation include the coordination of cell signals and the activity of post-transcriptional factors. MicroRNAs (miRNAs/miRs) serve an important role in osteoblastic differentiation. miRNAs are small non-coding single-stranded RNAs that inhibit the translation or promote the degradation of target mRNAs through binding to their 3'-untranslated region (UTR), and thereby attenuate protein synthesis (6). Numerous miRNAs have been characterized in diverse biological and pathological processes, including cell proliferation, apoptosis, differentiation and tumorigenesis (7-10). There is also evidence that aberrant miRNA expression is strongly associated with osteoblast differentiation through various mechanisms (11). miR-877-3p has been demonstrated to promote cell proliferation and differentiation in lung and bladder cancer (12,13). In addition, miR-877-3p has been revealed to inhibit the myofibroblast differentiation of lung-resident mesenchymal stem cells and attenuate the lung fibrosis induced by bleomycin (12). However, it is unclear whether miR-877-3p is one of the key miRNAs that regulate the proliferation and differentiation of osteoblasts.

The aim of the present study was to define the role of miR-877-3p in osteoblast differentiation using MC3T3-E1 cells, an osteoblast precursor cell line derived from mouse calvaria that has been widely used as a model in bone biology research (14). Results demonstrated that miR-877-3p was upregulated during TGF-β1-mediated osteoblastic

differentiation. Bioinformatics analysis identified Smad7 as a target of miR-877-3p. Osteoblastic differentiation of MC3T3-E1 cells was induced by miR-877-3p overexpression whilst Smad7 overexpression partially reversed this effect. Therefore, miR-877-3p/Smad7 may represent a potential therapeutic target for bone regeneration-associated diseases.

Materials and methods

Cell culture and osteoblastic differentiation. The MC3T3-E1 cell line was obtained from the Chinese Academy of Sciences Cell Bank (Shanghai, China) and cultured in α-minimal essential medium (α-MEM; Gibco; Thermo Fisher Scientific, Inc., Waltham, MA, USA) containing penicillin (50 U/ml), 10% fetal bovine serum (Gibco; Thermo Fisher Scientific, Inc.) and streptomycin (50 μg/ml) at 37°C in a humidified atmosphere with 5% CO_2. For TGF-β1 treatment, recombinant human TGF-β1 (cat. no. CSB-AP003861HU; CUSABIO Technology LLC, Wuhan, China) with final concentration of 4 ng/ml was added to cell culture for 7 or 14 days. To induce osteoblastic differentiation, cells were seeded ($1x10^5$ cells per well) in 6-well plates and treated with osteogenic medium (10 ng/ml β-glycerophosphate; 10 mmol/l dexamethasone and 50 μg/ml vitamin C; all from Sigma-Aldrich; Merck KGaA) for 7 and 14 days when they reached 70% confluence (15).

Cell transfection. pcDNA3.1-Smad negative control (NC) and pcDNA3.1-Smad7 were synthesized by GenePharma Co., Ltd. (Jiangsu, China). miR-877-3p mimics, inhibitor and their corresponding negative controls (NCs), miR-877-3p agomir, miR-877-3p antagomir and their corresponding controls (mimics NC: miR01101, RiboBio Co., Ltd., and inhibitor NC; miR02101; RiboBio Co., Ltd.) were synthesized by Guangzhou RiboBio Co., Ltd. (Guangzhou, China). The sequences were as follows: miR-877-3p mimics, 5'-UGUCCUCUUCUCCCU CCUCCCA-3'; miR-877-3p inhibitor, 5'-UGGGAGGAGGGA GAAGAGGACA-3'; miR-877-3p agomir, 5'-UGUCCUCUU CUCCCUCCUCCCA-3' and miR-877-3p antagomir, 5'-UGG GAGGAGGGAGAAGAGGACA-3'. MC3T3-E1 cells were seeded in 6-well plates at a density of 30,000 cells/well and cultured for 24 h in antibiotic-free fresh medium. Subsequently, the cells were transfected with miRNA or vector (100 nM) using Lipofectamine 3000 (Invitrogen; Thermo Fisher Scientific, Inc.) according to the manufacturer's protocol. After 48 h incubation, the cells were used for further experiments.

RNA isolation and RT-qPCR. Total RNA was extracted from cells or tissue with TRIzol reagent (Invitrogen; Thermo Fisher Scientific, Inc.) according to the manufacturer's protocol. Total RNA was quantified by Nanodrop 2000 spectrophotometry (Thermo Fisher Scientific, Inc.). First-strand cDNA synthesis was then performed using a Superscript RT kit (Biouniquer Technology, Nanjing, China) following the manufacturer's instructions. The reaction was performed under the following conditions: 37°C for 15 min and 98°C for 5 min. qPCR was conducted with SYBR Green I (Biouniquer Technology) using the LightCycler 480 II System (Roche Diagnostics, Basel, Switzerland). Primer sequences were as follows: miR-877-3p-F, 5'-GCGTGTATTTGACAAGCTGAGTTG-3'; collagen type I α1 chain (COL1A1) forward, 5'-TCGTGGTGAGAC

TGGTCCTG-3' and reverse, 5'-TGTCACCTTGTTCGCCTG TC-3'; runt-related transcription factor 2 (RUNX2) forward, 5'-CGGACGAGGCAAGAGTTTC-3' and reverse, 5'-TGG CTCAGATAGGAGGGGTAA-3'; osterix (OSX) forward, 5'-AGCAGCAGCAGCAACAGAAG-3' and reverse, 5'-CTC AGGCCAGCTCACTCTTG-3'; Smad7 forward, 5'-GCTATT CCAGAAGATGCTGTTC-3' and reverse, 5'-GTTGCTGAG CTGTTCTGATTTG-3'; β-actin forward 5'-GTCCCTCAC CCTCCCAAAAG-3' and reverse, 5'-GCTGCCTCAACACCT CAACCC-3'. The thermocycling conditions were as follows: 95°C for 5 min, followed by 35 cycles at 95°C for 10 sec then 60°C for 30 sec. The $2^{-\Delta\Delta Cq}$ method was used for data analysis with normalization to β-actin (16). U6 (cat. no. B532461-0001; Sangon Biotech Co., Ltd., Shanghai, China) was used as endogenous control for the analysis of miR-877-3p expression.

Measurement of alkaline phosphatase (ALP) activity. Total proteins were extracted from cells using a radioimmunoprecipitation assay (RIPA) lysis buffer (Biouniquer Technology) and quantified by bicinchoninic acid assay according to the manufacturer's protocol. The cell lysate was added to 96-well plates and incubated with ALP staining solution (Sigma-Aldrich; Merck KGaA) for 60 min at 37°C. Following the addition of the stop solution, ALP activity was measured spectrophotometrically at 405 nm, and normalized to the total protein concentration.

Mineralization assay. The MC3T3-E1 cells were cultured with TGF-β1 (4 ng/ml) and osteoblastic differentiation medium for 7 days in 24-well plates at a density of $2x10^4$ cells per well, and the mineralization of the MC3T3-E1 cells was observed via Alizarin Red S (ARS) and ALP staining with an optical light microscope (ARS, Solarbio, China; ALP staining kit, Beyotime Institute of Biotechnology, Haimen, China).

In vivo transplantation. A total of 24 female NOD/SCID mice (age, 4 weeks; weight, 17-19 g) were purchased from the Provincial Animal Center (Guangdong, China) and housed for 1 week to adapt them to the laboratory environment (24°C, 12-h light/dark cycles and humidity 60±10%) with free access to water and food. The mice were randomly divided into four groups (each n=6). MC3T3-E1 cells transfected with miR-877-3p mimics, miR-877-3p mimics inhibitor or their corresponding controls were induced with osteogenic medium for 14 days *in vitro*. Then, $5x10^6$ cells were loaded onto 20 mg hydroxyapatite-tricalcium phosphate (Sigma-Aldrich; Merck KGaA) and subcutaneously implanted in the dorsal region of the NOD/SCID mice. When the xenografts reached 50 mm³ in volume, miR-877-3p agomir or antagomir or their corresponding controls (5 nmol), respectively, was injected into the tumor every other day. Four weeks later, the xenografts were removed, fixed with 4% paraformaldehyde for 3 days and then decalcified in 10% EDTA (pH 6.0) for 7 days. The xenografts were then embedded in paraffin, sectioned (4 μm) and stained with hematoxylin and eosin (H&E), or Masson's trichrome stain (Sigma-Aldrich; Merck KGaA) according to the manufacturer's protocols. All animal procedures were approved by the Animal Care Committee of Southern Medical University (L2016113).
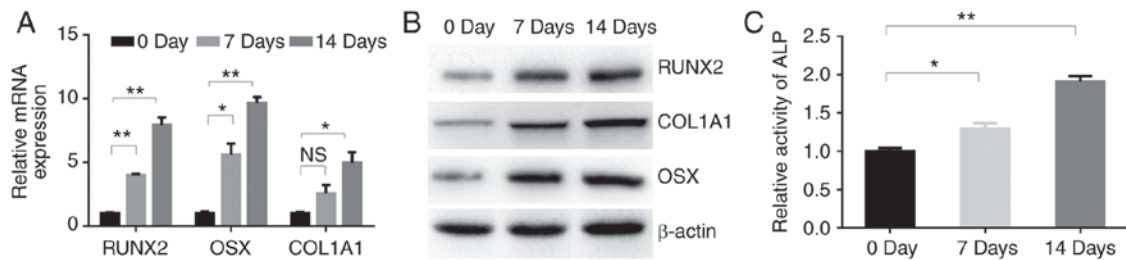
Figure 1. TGF-β1 promotes the osteoblastic differentiation of MC3T3-E1 cells. (A) RT-qPCR analysis of the osteogenic-related genes RUNX2, OSX and COL1A1 in MC3T3-E1 cells after treatment with TGF-β1 (4 ng/ml) for 0, 7 and 14 days. (B) Western blotting of RUNX2, COL1A1-and OSX protein in MC3T3-E1 cells cultured with TGF-β1 (4 ng/ml) for 0, 7 and 14 days. (C) ALP activity in MC3T3-E1 cells after treatment with TGF-β1 (4 ng/ml) for 0, 7 and 14 days. NS, no significance change; *P<0.05, **P<0.01 as indicated. TGF, transforming growth factor; RUNX2, runt-related transcription factor 2; OSX, osterix; COL1A1 collagen type I α1 chain; ALP, alkaline phosphatase.

Western blotting. The cells were harvested and lysed with RIPA buffer (Beyotime Institute of Biotechnology) containing phenylmethane sulfonyl fluoride and protease inhibitors. Equal amounts of protein (30 μg per lane) were loaded on a 10% sodium dodecyl sulfate-polyacrylamide gel, separated by electrophoresis, and transferred onto a 0.4-μm polyvinylidene difluoride membrane (EMD Millipore, Billerica, MA, USA). The membranes were sealed with 5% non-fat milk for 1 h at room temperature, then incubated with primary antibodies overnight at 4˚C. The primary antibodies were anti-Smad7 (1:100; cat. no. sc-365846, Santa Cruz Biotechnology, Ltd., Dallas, TX, USA), anti-OSX (1:200; cat. no. sc-393325, Santa Cruz Biotechnology, Ltd.), anti-COL1A1 (1:1,000; cat. no. ab90395, Abcam, Cambridge, UK), anti-RUNX2 (1:1,000; cat. no. 12556; Cell Signaling Technology, Inc., Danvers, MA, USA), anti-phospho-Smad2 (1:1,000; cat. no. 18338; Cell Signaling Technology, Inc.), anti-Smad2 (1:1,000; cat. no. 5339; Cell Signaling Technology, Inc.), anti-phospho-Smad3 (1:1,000; cat. no. ab52903; Abcam, Cambridge, UK), Smad3 (1:1,000; cat. no. 9523, Cell Signaling Technology, Inc.) and anti-β-actin antibody (1:1,000; cat. no. 4970; Cell Signaling Technology, Inc.). The membranes were probed with horseradish peroxidase-conjugated anti-rabbit secondary antibody for 1 h at room temperature (1:5,000; cat. no. 7074; Cell Signaling Technology, Inc.) and the protein signals were obtained with ECL Plus substrate (EMD Millipore).

Luciferase reporter assay. The wild-type and mutant putative miR-877-3p binding sites in the 3'UTR of Smad7 were synthesized and cloned into a pmirGLO luciferase vector (Shanghai Genechem Co., Ltd., Shanghai, China). The plasmids, miRNA (miR-877-3p and miR-NC) and Renilla luciferase plasmid (Shanghai Genechem Co., Ltd.) were co-transfected into cells using Lipofectamine 3000 (Invitrogen; Thermo Fisher Scientific, Inc.). Firefly and *Renilla* luciferase activities were then measured using the Dual Luciferase Reporter Assay system (Promega Corporation, Madison, WI, USA) at 48 h after transfection. All experiments were repeated three times.

Bioinformatics target prediction. The candidate target genes of miR-877-3p were predicted using TargetScan online software (http://www.targetscan.org/).

Statistical analysis. Data are expressed as mean ± standard deviation and were analyzed using SPSS 22.0 software (IBM Corp., Armonk, NY, USA). All experiments were repeated at least three times with comparable results unless indicated otherwise. Statistical evaluation of the data was performed using the unpaired Student's t-test for comparisons between two groups and one-way analysis of variance followed by Bonferroni correction post hoc test for comparisons amongst multiple groups. P<0.05 was considered to indicate a statistically significant difference.

Results

TGF-β1 promotes the osteoblastic differentiation of MC3T3-E1 cells. To induce osteoblastic differentiation, the MC3T3-E1 cells were treated with TGF-β1. The mRNA expression levels of three osteogenic genes, namely RUNX2, OSX and COL1A1, were then determined in the MC3T3-E1 cells at 0, 7 and 14 days after TGF-β1 treatment. The expression levels of RUNX2, OSX and COL1A1 mRNA in the MC3T3-E1 cells were increased at days 7 and 14 compared with the respective levels at day 0, with the highest levels being observed at day 14 (Fig. 1A). Consistently, the corresponding protein levels in the MC3T3-E1 cells appeared to increase in a time-dependent manner (Fig. 1B). Furthermore, ALP activity gradually increased during treatment with TGF-β1 (Fig. 1C), indicating the key role of TGF-β1 in osteoblastic differentiation.

Expression of miR-877-3p is significantly altered during osteoblast induction and promotes the osteoblastic differentiation of MC3T3-E1 cells. The role of miR-877-3p during osteoblast differentiation is unclear. Therefore, the aim of the present study was to investigate whether miR-877-3p is associated with osteogenic differentiation. Following the treatment of MC3T3-E1 cells with TGF-β1, the expression of miR-877-3p was detected using RT-qPCR analysis, and a time-dependent increase in the level of miR-877-3p was observed (Fig. 2A). To further elucidate the functional role of miR-877-3p during osteoblastic differentiation, miR-877-3p was overexpressed and knocked down in MC3T3-E1 cells via transfection with miR-877-3p mimics and miR-877-3p inhibitor, respectively, and corresponding controls were established for comparison (Fig. 2B). The mRNA levels of the osteoblast-associated markers RUNX2, OSX and COL1A1 were found to be significantly elevated in miR-877-3p-overexpressing MC3T3-E1 cells, and significantly reduced in
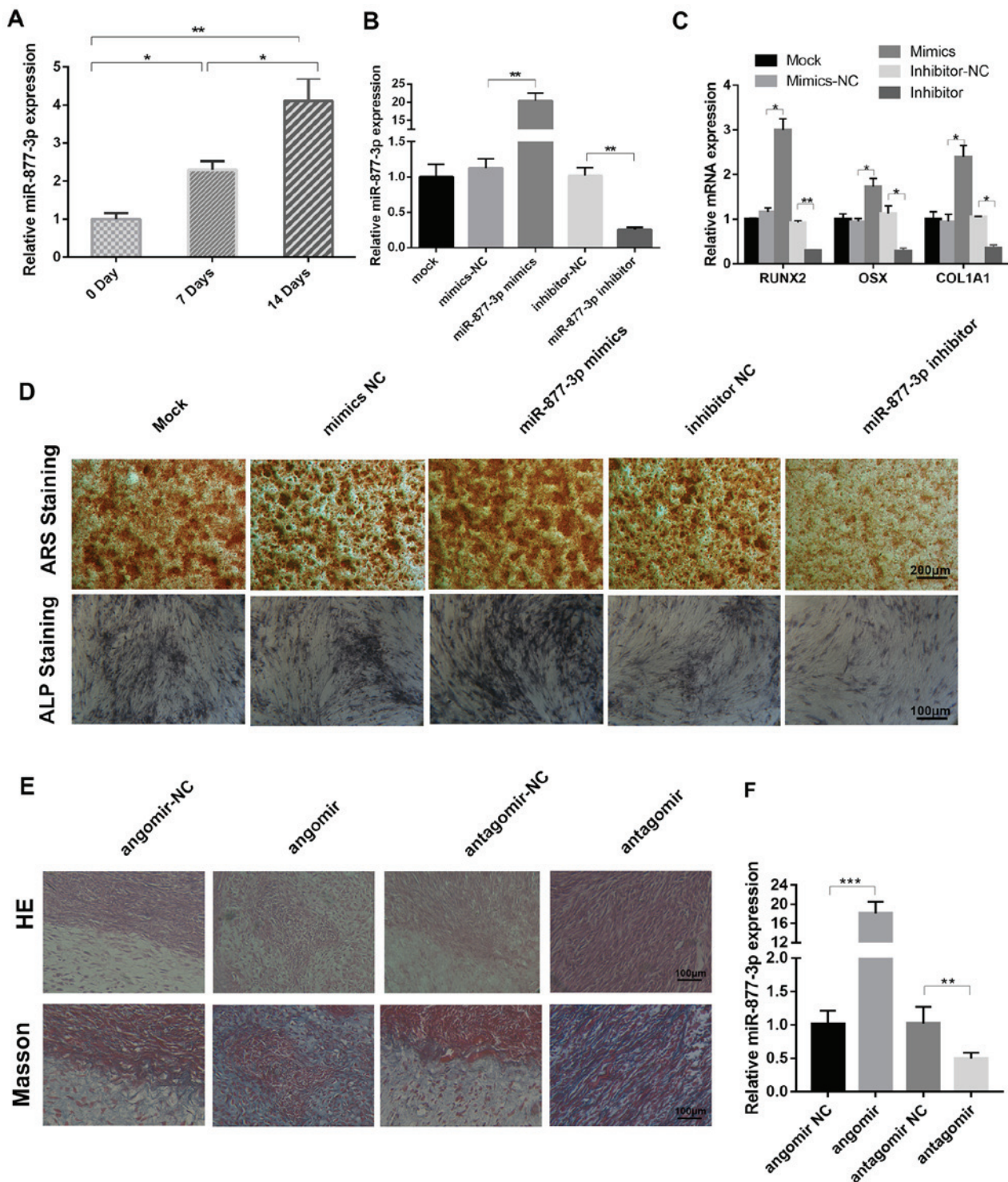
Figure 2. miR-877-3p promotes the osteoblastic differentiation of MC3T3-E1 cells. (A) miR-877-3p expression in MC3T3-E1 cells after treatment with TGF-β1 (4 ng/ml) for 0, 7 and 14 days. (B) Expression of miR-877-3p was validated in MC3T3-E1 cells transfected with miR-877-3p mimics or inhibitor and their corresponding controls by RT-qPCR. (C) RUNX2, OSX and COL1A1 mRNA expression in MC3T3-E1 cells. (D) MC3T3-E1 cells transfected with miR-877-3p mimics or inhibitor and their corresponding controls were cultured in osteogenic medium. At day 14, the mineralization of differentiated MC3T3-E1 cells was detected with ARS and ALP staining. (E) Transfected MC3T3-E1 cells were cultured in osteogenic medium for 14 days and then mixed with tricalcium phosphate/hydroxyapatite and transplanted into the dorsal region of nude mice for 4-weeks. The results were then evaluated by H&E and Masson's trichrome staining. (F) (F) Transfected MC3T3-E1 cells were cultured in osteogenic medium for 14 days and then mixed with tricalcium phosphate/hydroxyapatite and transplanted into the dorsal region of nude mice for 4-weeks. The Expression expression of miR-877-3p in the xenografts from each group was detected by RT-qPCR analysis. *P<0.05, **P<0.01 and ***P<0.001, as indicated. miR, microRNA; TGF, transforming growth factor; RUNX2, runt-related transcription factor 2; OSX, osterix; COL1A1 collagen type I α1 chain; NC, negative control; ARS, Alizarin Red S; ALP, alkaline phosphatase; H&E, hematoxylin and eosin.

cells with miR-877-3p knockdown (Fig. 2C). Consistently, ARS and ALP staining results demonstrated that the staining intensity of mineralization nodes was markedly increased in the miR-877-3p-overexpressing cells, and decreased in the
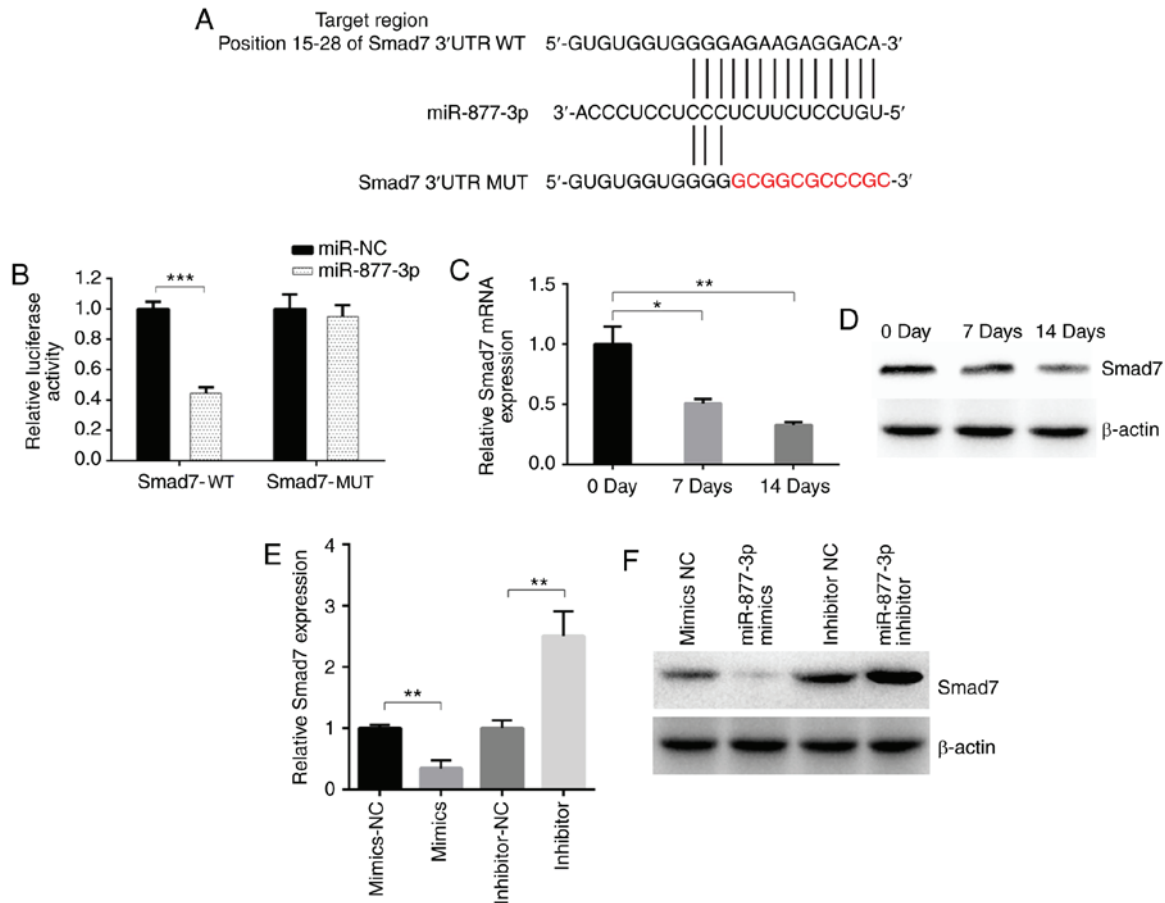
Figure 3. miR-877-3p inhibits the expression of Smad7. (A) Design of luciferase reporters with the WT Smad7 3'UTR or the site-directed MUT Smad7 3'UTR. (B) Effect of miR-877-3p and miR-NC on luciferase activity in MC3T3-E1 cells transfected with the WT or MUT Smad7 3'UTR. Smad7 expression detected by (C) RT-qPCR and (D) western blotting in MC3T3-E1 cells after culture with TGF-β1 (4 ng/ml) for 0, 7 and 14 days. Smad7 (E) mRNA and (F) protein expression in MC3T3-E1 cells transfected with miR-877-3p mimics or inhibitors and their corresponding controls. *P<0.05, **P<0.01 as indicated. miR, microRNA; WT, wild type; MUT, mutant; UTR, untranslated region; NC, negative control; TGF, transforming growth factor.

miR-877-3p-depleted cells (Fig. 2D). The effect of miR-877-3p on MC3T3-E1 osteogenesis was further evaluated *in vivo*. The H&E and Masson's trichrome staining results revealed that osteoid formation was increased in the xenografts of mice treated with miR-877-3p agomir, and decreased in those of the mice treated with miR-877-3p antagomir (Fig. 2E). RT-qPCR analysis confirmed that the expression of miR-877-3p was elevated in the agomir-treated group and reduced in antagomir-treated group, compared with the respective controls (Fig. 2F). These results demonstrate that miR-877-3p promoted the osteogenic differentiation of MC3T3-E1 cells.

MiR-877-3p inhibits the expression of Smad7. miR-877-3p has been demonstrated to promote the TGF-β1-induced osteoblastic differentiation of MC3T3-E1 cells; however, its downstream target has not yet been determined. Using the online bioinformatics tool TargetScan, Smad7 was predicted to be a downstream target of miR-877-3p with a potential binding site (Fig. 3A). Fragments of the 3'UTR of Smad7 containing a putative miR-877-5p binding site or mutant fragment were synthesized and inserted into plasmids. The predicted binding site of miR-877-3p in Smad7 was confirmed using a luciferase reporter assay (Fig. 3B). The mRNA and protein levels of Smad7 were decreased after TGF-β1 induction

(Fig. 3C and D). Whether miR-877-3p regulated osteogenic differentiation by suppressing Smad7 expression was then investigated. The results revealed a notable downregulation of Smad7 expression following the transfection of miR-877-3p mimic into MC3T3-E1 cells, whereas Smad7 was upregulated in cells transfected with miR-877-3p inhibitor, as confirmed by RT-qPCR and western blot assays (Fig. 3E and F). These results support the hypothesis that miR-877-3p directly binds to Smad7.

Smad7 may be a negative target of miR-877-3p involved in osteoblast differentiation. Although Smad7 expression has been found to be affected by miR-877-3p, the interaction between Smad7 and miR-877-3p required further evaluation. To confirm the role of the miR-877-3p/Smad7 axis in the regulation of osteoblastic differentiation, MC3T3-E1 cells transfected with miR-877-3p inhibitor or inhibitor-NC were cultured with or without TGF-β1 for 7 days. Compared with the control cells transfected with inhibitor-NC, the expression of Smad7 was upregulated when cells were transfected with miR-877-3p inhibitor alone, while TGF-β1 reversed the expression of Smad7 induced by the miR-877-3p inhibitor, as confirmed by RT-qPCR (Fig. 4A). By contrast, the osteogenesis-associated genes RUNX2, OSX and COL1A1
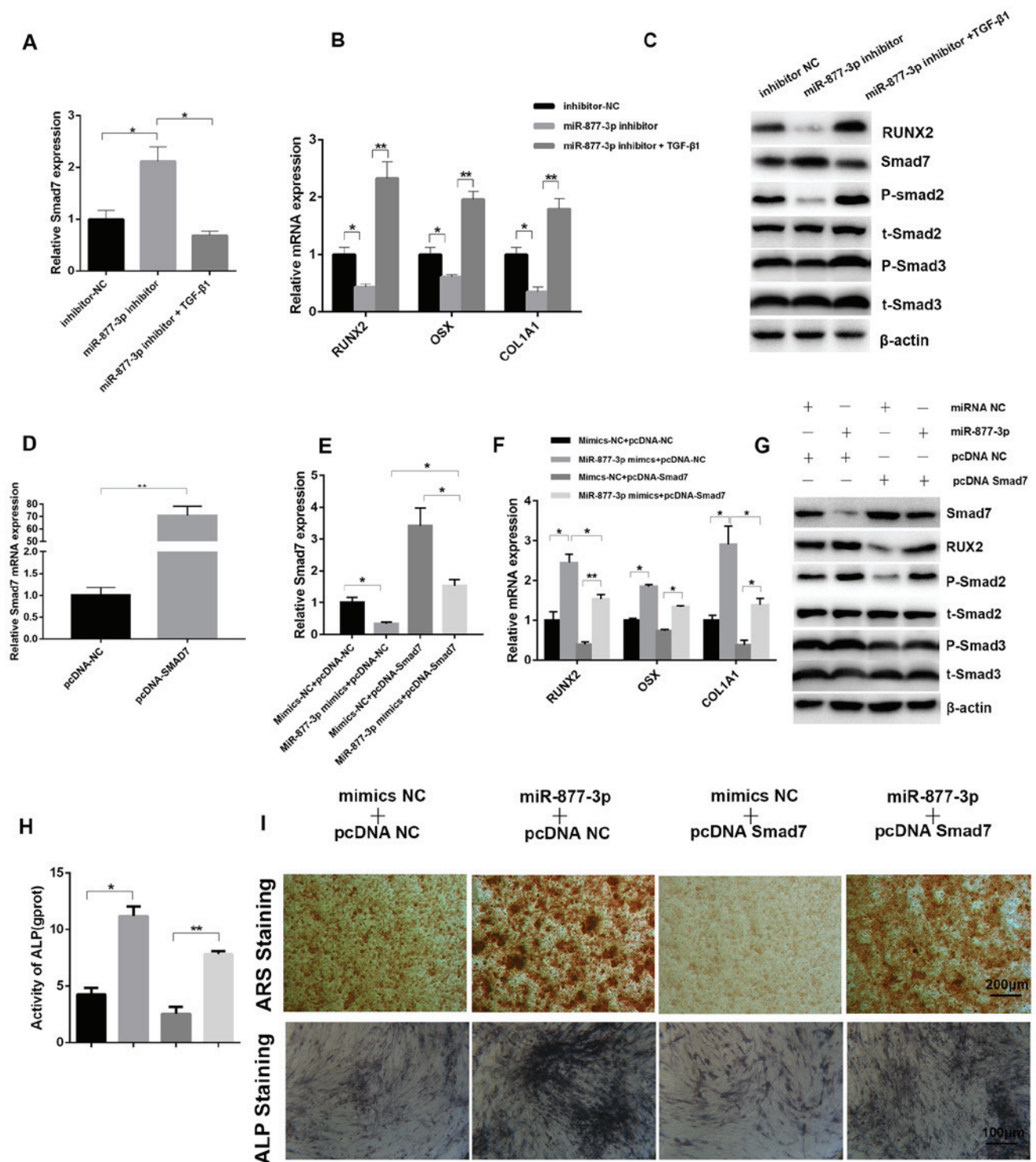
Figure 4. Smad7 is identified as a downstream target of miR-877-3p during the osteoblastic differentiation of MC3T3-E1 cells. mRNA expression of (A) Smad7 and (B) osteoblast differentiation-associated genes in MC3T3-E1 cells transfected with inhibitor-NC, miR-877-3p inhibitor or miR-877-3p inhibitor plus TGF-β1. (C) Expression of RUNX2, Smad7, p-Smad2, t-Smad2, p-Smad3 and t-Smad3 protein in MC3T3-E1 cells transfected with inhibitor-NC, miR-877-3p inhibitor or miR-877-3p inhibitor plus TGF-β1. (D) The mRNA expression of Smad7 was validated in MC3T3-E1 cells transfected with pcDNA-NC or pcDNA-Smad7. The mRNA expression of (E) Smad7 and (F) osteoblast differentiation-associated genes in MC3T3-E1 cells transfected with miR-877-3p mimics and/or pcDNA-Smad7. (G) Protein levels of Smad7, RUNX2, p-Smad2, t-Smad2, p-Smad3 and t-Smad3 in MC3T3-E1 cells transfected with miR-877-3p mimics and/or pcDNA-Smad7. (H) ALP activity of MC3T3-E1 cells transfected with miR-877-3p mimics and/or pcDNA-Smad7 after culture with osteogenic medium for 7 days. (I) MC3T3-E1 cells transfected with miR-877-3p mimics and/or pcDNA-Smad7 were induced with osteogenic medium. At day 14, the mineralization of differentiated MC3T3-E1 cells was detected with ARS and ALP staining. $^*P<0.05$, $^{**}P<0.01$ as indicated. miR, microRNA; NC, negative control; TGF, transforming growth factor; RUNX2, runt-related transcription factor 2; p, phospho; t, total; ALP, alkaline phosphatase; ARS, Alizarin Red S.

exhibited the opposite tendency (Fig. 4B). The protein levels of RUNX2 and Smad7 were also verified by western blotting, and were consistent with the mRNA results. Western blotting also revealed that the levels of phospho-Smad2 and phospho-Smad3 were decreased by the miR-877-3p inhibitor, and this effect was reversed by TGF-β1 (Fig. 4C). Furthermore,

Smad7-overexpressing and control MC3T3-E1 cells were established by transfection with a pcDNA3.1-Smad7 plasmid (pcDNA-Smad7) and control plasmid (pcDNA-NC), and then co-transfected with miR-877-3p mimics or mimics-NC, and the success of transfection was verified using RT-qPCR (Fig. 4D and E). The promoting effects of miR-877-3p mimics on osteogenesis-related genes, phospho-Smad2 and phospho-Smad3 were markedly inhibited by pcDNA-Smad7 (Fig. 4F and G). ALP activity, ARS and ALP staining exhibited the same tendency (Fig. 4H and I). Collectively, these results confirmed that Smad7 inhibits the osteoblastic differentiation of MC3T3-E1 cells and is able to reverse the osteoblastic differentiation mediated by miR-877-3p.

Discussion

Bone formation and mineralization are triggered by the differentiation of mesenchymal precursor cells into osteo-blasts. Osteoblast differentiation is significantly affected by a key transcriptional factor, RUNX2, that regulates the expression of several osteogenic genes, including ALP, OSX and COL1A1 (17-19). These osteogenic genes are associated with the expression of bone matrix genes such as type 1 collagen, osteopontin, osteocalcin and bone sialoprotein (20-23). In addition, several signaling pathways, including Wnt/β-catenin, BMP/TGF-β, JAK/STAT and MAPK, have been reported to promote osteoblast differentiation *in vivo* and *in vitro* (23-25). TGF-β1 is a polypeptide member of the TGF-β superfamily of cytokines that regulate several cellular functions, including cell proliferation, survival and differentiation (26-28). The combined actions of these biological processes rely on the effect of TGF-β1 on bone formation (29).

MC3T3-E1 cells, which are mouse pre-osteoblast cells considered to be good models for the study of *in vitro* osteoblast differentiation (14), were used in the present study. These cells were treated with TGF-β1 to induce osteoblastic differentiation, which was evaluated by the expression of the aforementioned osteoblast gene markers. It must be acknowledged that a limitation of the present study is that only one cell line was investigated; different cell lines, such as primary osteoblasts, should be included in further studies. However, the experiments in the present study were, to the best of our knowledge, the first to provide evidence that miR-877-3p is upregulated during the osteoblastic differentiation of MC3T3-E1 cells in a time-dependent manner. Consistent with this observation, miR-877-3p has also been found to be highly upregulated during myofibroblast differentiation (12). Subsequently, the effect of miR-877-3p on TGF-β1-induced osteoblast differentiation and mineralization was investigated, by overexpression and knockdown experiments performed in the osteoblast cell line. The results clearly demonstrated that miR-877-3p promotes osteoblast differentiation.

miRNAs have been identified as post-transcriptional inhibitors that exert their biological effects via the downregulation of target gene expression. Bioinformatics analysis in the present study identified Smad7 as a putative target of miR-877-3p. By transient transfection with miR-877-3p mimics or inhibitor, it was demonstrated that miR-877-3p suppressed Smad7 mRNA and protein expression in MC3T3-E1 cells. Smad7 is a well-defined negative

regulator of the TGF-β1 signaling pathway and bone metabolism (30). As regards to bone formation initiated by osteoblasts, decreasing expression of Smad7 during osteoblast differentiation of MC3T3-E1 cells was observed in the present study, which is consistent with previously reported findings (31). The present study also indicated that the expression of Smad7 increased in MC3T3-E1 cells with miR-877-3p downregulation, while this effect was eliminated in the presence of TGF-β1. Therefore, it was hypothesized that Smad7 is a negative target of miR-877-3p and TGF-β1, and that one of the important mechanisms by which miR-877-3p promotes the osteoblastic differentiation induced by TGF-β1 may be through suppressing the expression of the Smad7 gene. This hypothesis was confirmed in the co-transfection experiment. The results suggested that overexpression of Smad7 partially inhibited the miR-877-3p-mediated osteoblastic differentiation of MC3T3-E1 cells. However, evidence is required to demonstrate that microRNAs-877-3p regulate osteoblast differentiation by interacting with Smad7. In addition, the role of miRNAs in osteoblast differentiation is complex; the bypass or crosstalk of microRNAs-877-3p in this process was not excluded, and requires further study.

In summary, the results of the present study revealed the mechanism underlying the regulatory effect of miR-877-3p on the osteoblastic differentiation of MC3T3-E1 cells. Through this mechanism, miR-877-3p promoted osteoblastic differentiation of MC3T3-E1 cells induced by TGF-β1 via silencing Smad7. These findings provided novel insights into the effects of miR-877-3p on osteoblast differentiation and bone formation, which may provide a new therapeutic approach for degenerative bone diseases.

Availability of data and materials

All data generated or analyzed during the present study are available from the corresponding author upon reasonable request.

Authors' contributions

DH conceived and designed the experiments, conducted the data analysis, contributed reagents/materials/tools and wrote the manuscript. GH and JC performed the experiments. All authors read and approved the final manuscript. All authors contributed to the data analysis, drafting and critical revision of the paper, and agree to be accountable for all aspects of the work.

Ethics approval and consent to participate

All animal procedures were approved by the Animal Care Committee of Southern Medical University (L2016113).

Patient consent for publication

Not applicable.

Competing interests

The authors declare that they have no competing interests.

References

1. Takayanagi H: Osteoimmunology: Shared mechanisms and crosstalk between the immune and bone systems. Nat Rev Immunol 7: 292-304, 2007.
2. Manolagas SC and Jilka RL: Bone marrow, cytokines, and bone remodeling. Emerging insights into the pathophysiology of osteoporosis. N Engl J Med 332: 305-311, 1995.
3. Bernabeu C, Lopez-Novoa JM and Quintanilla M: The emerging role of TGF-beta superfamily coreceptors in cancer. Biochim Biophys Acta 1792: 954-973, 2009.
4. Crane JL, Xian L and Cao X: Role of TGF-β signaling in coupling bone remodeling. Methods Mol Biol 1344: 287-300, 2016.
5. Yasui T, Kadono Y, Nakamura M, Oshima Y, Matsumoto T, Masuda H, Hirose J, Omata Y, Yasuda H, Imamura T, *et al*: Regulation of RANKL-induced osteoclastogenesis by TGF-β through molecular interaction between Smad3 and Traf6. J Bone Miner Res 26: 1447-1456, 2011.
6. Bartel DP: MicroRNAs: Genomics, biogenesis, mechanism, and function. Cell 116: 281-297, 2004.
7. Huang J, Zhao L, Xing L and Chen D: MicroRNA-204 regulates Runx2 protein expression and mesenchymal progenitor cell differentiation. Stem Cells 28: 357-364, 2010.
8. Xiang LY, Ou HH, Liu XC, Chen ZJ, Li XH, Huang Y and Yang DH: Loss of tumor suppressor miR-126 contributes to the development of hepatitis B virus-related hepatocellular carcinoma metastasis through the upregulation of ADAM9. Tumour Biol 39: 1010428317709128, 2017.
9. Cao M, Hou D, Liang H, Gong F, Wang Y, Yan X, Jiang X, Wang C, Zhang J, Zen K, *et al*: miR-150 promotes the proliferation and migration of lung cancer cells by targeting SRC kinase signalling inhibitor 1. Eur J Cancer 50: 1013-1024, 2014.
10. Chen JF, Mandel EM, Thomson JM, Wu Q, Callis TE, Hammond SM, Conlon FL and Wang DZ: The role of microRNA-1 and microRNA-133 in skeletal muscle proliferation and differentiation. Nat Genet 38: 228-233, 2006.
11. Taipaleenmäki H, Bjerre Hokland L, Chen L, Kauppinen S and Kassem M: Mechanisms in endocrinology: micro-RNAs: Targets for enhancing osteoblast differentiation and bone formation. Eur J Endocrinol 166: 359-371, 2012.
12. Wang C, Gu S, Cao H, Li Z, Xiang Z, Hu K and Han X: miR-877-3p targets Smad7 and is associated with myofibroblast differentiation and bleomycin-induced lung fibrosis. Sci Rep 6: 30122, 2016.
13. Li S, Zhu Y, Liang Z, Wang X, Meng S, Xu X, Xu X, Wu J, Ji A, Hu Z, *et al*: Up-regulation of p16 by miR-877-3p inhibits proliferation of bladder cancer. Oncotarget 7: 51773-51783, 2016.
14. Niu YB, Kong XH, Li YH, Fan L, Pan YL, Li CR, Wu XL, Lu TL and Mei QB: Radix Dipsaci total saponins stimulate MC3T3-E1 cell differentiation via the bone morphogenetic protein-2/MAPK/Smad-dependent Runx2 pathway. Mol Med Rep 11: 4468-4472, 2015.
15. Wang L, Wu F, Song Y, Li X, Wu Q, Duan Y and Jin Z: Long noncoding RNA related to periodontitis interacts with miR-182 to upregulate osteogenic differentiation in periodontal mesenchymal stem cells of periodontitis patients. Cell Death Dis 7: e2327, 2016.
16. Livak KJ and Schmittgen TD: Analysis of relative gene expression data using real-time quantitative PCR and the 2(-Delta Delta C(T)) method. Methods 25: 402-408, 2001.
17. Dacic S, Kalajzic I, Visnjic D, Lichtler AC and Rowe DW: Col1a1-driven transgenic markers of osteoblast lineage progression. J Bone Miner Res 16: 1228-1236, 2001.
18. Nakashima K, Zhou X, Kunkel G, Zhang Z, Deng JM, Behringer RR and de Crombrugghe B: The novel zinc finger-containing transcription factor osterix is required for osteoblast differentiation and bone formation. Cell 108: 17-29, 2002.
19. Pratap J, Galindo M, Zaidi SK, Vradii D, Bhat BM, Robinson JA, Choi JY, Komori T, Stein JL, Lian JB, *et al*: Cell growth regulatory role of Runx2 during proliferative expansion of preosteoblasts. Cancer Res 63: 5357-5362, 2003.
20. Baek WY and Kim JE: Transcriptional regulation of bone formation. Front Biosci (Schol Ed) 3: 126-135, 2011.
21. Bruderer M, Richards RG, Alini M and Stoddart MJ: Role and regulation of RUNX2 in osteogenesis. Eur Cell Mater 28: 269-286, 2014.
22. Ohata Y and Ozono K: Bone and stem cells. The mechanism of osteogenic differentiation from mesenchymal stem cell. Clin Calcium 24: 501-508, 2014 (In Japanese).
23. Bodine PV and Komm BS: Wnt signaling and osteoblastogenesis. Rev Endocr Metab Disord 7: 33-39, 2006.
24. Levy JB, Schindler C, Raz R, Levy DE, Baron R and Horowitz MC: Activation of the JAK-STAT signal transduction pathway by oncostatin-M cultured human and mouse osteoblastic cells. Endocrinology 137: 1159-1165, 1996.
25. Beederman M, Lamplot JD, Nan G, Wang J, Liu X, Yin L, Li R, Shui W, Zhang H, Kim SH, *et al*: BMP signaling in mesenchymal stem cell differentiation and bone formation. J Biomed Sci Eng 6: 32-52, 2013.
26. Massagué J, Blain SW and Lo RS: TGFbeta signaling in growth control, cancer, and heritable disorders. Cell 103: 295-309, 2000.
27. Park JS, Chu JS, Tsou AD, Diop R, Tang Z, Wang A and Li S: The effect of matrix stiffness on the differentiation of mesenchymal stem cells in response to TGF-β. Biomaterials 32: 3921-3930, 2011.
28. Siegel PM and Massagué J: Cytostatic and apoptotic actions of TGF-beta in homeostasis and cancer. Nat Rev Cancer 3: 807-821, 2003.
29. Janssens K, ten Dijke P, Janssens S and Van Hul W: Transforming growth factor-beta1 to the bone. Endocr Rev 26: 743-774, 2005.
30. Zhang F, Ren CC, Liu L, Chen YN, Yang L and Zhang XA: HOXC6 gene silencing inhibits epithelial-mesenchymal transition and cell viability through the TGF-β/smad signaling pathway in cervical carcinoma cell. Cancer Cell Int 18: 204, 2018.
31. Yano M, Inoue Y, Tobimatsu T, Hendy G, Canaff L, Sugimoto T, Seino S and Kaji H: Smad7 inhibits differentiation and mineralization of mouse osteoblastic cells. Endocr J 59: 653-662, 2012.